Inorganic Chemistry

Article

pubs.acs.org/IC

Silver(I) Complex Formation with Cysteine, Penicillamine, and Glutathione

Bonnie O. Leung, Farideh Jalilehvand,* Vicky Mah, Masood Parvez, and Qiao Wu

Department of Chemistry, University of Calgary, Calgary, Alberta T2N 1N4, Canada

Supporting Information

ABSTRACT: The complex formation between silver(I) and cysteine (H_2Cys), penicillamine (H_2Pen), and glutathione (H_3Glu) in alkaline aqueous solution was examined using extended X-ray absorption fine structure (EXAFS) and ^{109}Ag NMR spectroscopic techniques. The complexes formed in 0.1 mol dm^{-3} Ag(I) solutions with cysteine and penicillamine were investigated for ligand/Ag(I) (L/Ag) mole ratios increasing from 2.0 to 10.0. For the series of cysteine solutions (pH 10−11) a mean Ag−S bond distance of 2.45 ± 0.02 Å consistently emerged, while for penicillamine (pH 9) the average Ag−S bond distance gradually increased from 2.40 to 2.44 ± 0.02 Å. EXAFS and ^{109}Ag NMR spectra of a concentrated Ag(I)−cysteine solution ($C_{Ag(I)}$ = 0.8 mol dm^{-3}, L/Ag = 2.2) showed a mean Ag−S bond distance of 2.47 ± 0.02 Å and $\delta(^{109}Ag)$ 1103 ppm, consistent with prevailing, partially oligomeric AgS_3 coordinated species, while for penicillamine ($C_{Ag(I)}$ = 0.5 mol dm^{-3}, L/Ag = 2.0) the mean Ag−S bond distance of 2.40 ± 0.02 Å and $\delta(^{109}Ag)$ 922 ppm indicate that mononuclear AgS_2 coordinated complexes dominate. For Ag(I)−glutathione solutions ($C_{Ag(I)}$ = 0.01 mol dm^{-3}, pH ∼11), mononuclear AgS_2 coordinated species with a mean Ag−S bond distance of 2.36 ± 0.02 Å dominate for L/Ag mole ratios from 2.0 to 10.0. The crystal structure of the silver(I)−cysteine compound $(NH_4)Ag_2(HCys)(Cys)\cdot H_2O$ (**1**) precipitating at pH ∼10 was solved and showed a layer structure with both AgS_3 and AgS_3N coordination to the cysteinate ligands. A redetermination of the crystal structure of $Ag(HPen)\cdot H_2O$ (**2**) confirmed the proposed digonal AgS_2 coordination environment to bridging thiolate sulfur atoms in polymeric intertwining chains forming a double helix. A survey of Ag−S bond distances for crystalline Ag(I) complexes with *S*-donor ligands in different AgS_2, $AgS_2(O/N)$, and AgS_3 coordination environments was used, together with a survey of ^{109}Ag NMR chemical shifts, to assist assignments of the Ag(I) coordination in solution.

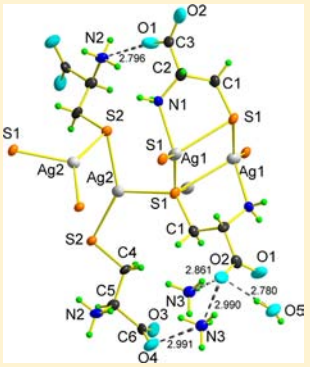

INTRODUCTION

Historical treatments with silver(I) salts as antiseptic agents are well documented.[1,2] Although the introduction of modern antibiotics greatly reduced the use of silver(I) in antimicrobial agents, the increasing bacterial resistance against antibiotics has renewed the interest,[3−5] with a rising number of reports on newer and more efficient silver-based antimicrobial biomaterials such as dressings,[6] gels,[7] and films.[8] Several studies show that the interaction between silver(I) ions and thiol-containing species such as cysteine (H_2Cys) and glutathione (H_3Glu) plays a key role in bacterial inactivation.[5,9] Silver nanoparticles also show antimicrobial properties;[10−14] it has been recently proposed that the mechanism of their action is via oxidation of Ag(0) atoms to Ag(I) ions under aerobic conditions.[15] Silver nanoparticles grafted with glutathione were also found to interfere with bacterial cell replication.[16] It has been proposed that soluble silver(I) ions can bind to thiol-containing amino acids in enzymes, such as NADH dehydrogenase. Ag(I) may also displace native metal ions from their natural binding sites in enzymes. Such interactions can interrupt the bacterial respiratory chain, leading to formation of reactive oxygen species that cause cell damage.[5,17,18]

For a better understanding of the broad-spectrum antimicrobial activity of silver ions, including effects on bacterial activity in the environment, and for developing more efficient antimicrobial silver(I) compounds, insight into the structural aspects of silver(I) complex formation with sulfur-containing amino acids and their derivatives is important. In the solid state, X-ray crystallographic studies reveal a tendency for silver(I) thiolates (RS^-) to form extended networks, where the steric hindrance of the ligand, stoichiometry, charge, and solvent play important roles in determining the degree of polymerization.[19] While X-ray powder diffraction patterns indicate layer structures for silver(I) complexes with primary alkane- and arenethiolates,[20] the steric interactions provided by secondary and tertiary alkanethiolate ligands favor formation of −S(R)−Ag−S(R)− ring structures with 3−14 Ag(I) ions.[21−24] Bulky thiol-containing ligands promote compact structures, with rings containing as few as three Ag−SR units, while less sterically hindered ligands form larger rings.[25] A survey in the Cambridge Structural Database (CSD) of crystalline silver(I) compounds with *S*-donor ligands (other than SCN^-) and AgS_2, AgS_2O, AgS_2N (except CN^-), or AgS_3 coordination is presented in Tables S1a−S1g in the Supporting Information and summarized in Table 1.[26]

Bell and co-workers reported that in the Ag(HPen) crystalline compound (H_2Pen = D-penicillamine, 3,3′-dimethyl-

Received: January 25, 2013
Published: April 4, 2013

   dx.doi.org/10.1021/ic400192c | *Inorg. Chem.* 2013, 52, 4593−4602

Table 1. Results of a CSD[26] Survey of Crystalline Silver(I) Complexes with *S*-Donor Ligands in AgS_2, $AgS_2(O/N)$, or AgS_3 Coordination[a]

Ag(I) coordination	no. of compds	range of Ag−S bond dist (Å)	av Ag−S bond dist (Å)[c]	range of Ag−(O/N) bond dist (Å)	av Ag−(O/N) bond dist (Å)[c]
AgS_2 (thiolates)	24	2.34−2.53	2.39 ± 0.03		
near-linear (≥170°)	18	2.34−2.45	2.39 ± 0.02		
AgS_2 (nonthiolates)	28	2.32−2.65	2.42 ± 0.05		
near-linear (≥170°)	16	2.36−2.65	2.42 ± 0.06		
AgS_2O[b]	16	2.41−2.59	2.47 ± 0.04	2.32−2.67	2.48 ± 0.18
AgS_2N (thiolates)	12	2.45−2.54	2.49 ± 0.02	2.22−2.36	2.29 ± 0.04
AgS_2N (nonthiolates)	14	2.43−2.87	2.54 ± 0.11	2.16−2.65	2.35 ± 0.15
AgS_3 (thiolates)	10	2.45−2.68	2.51 ± 0.05		
AgS_3 (nonthiolates)	37	2.40−2.87	2.53 ± 0.08		

[a]See Tables S1a−S1g in the Supporting Information. Thiocyanates and cyanides were omitted. [b]No thiolate *S*-donor ligands. [c]Population standard deviations are reported.

cysteine) obtained from a methanol/water mixture with a small amount of ammonia, bridging thiolate groups form polymeric −S(R)−Ag−S(R)−Ag− double chains with linear AgS_2 coordination in a double helix.[27] This structural feature is analogous to that described by Dance and co-workers for (3-methylpentane-3-thiolato)silver(I), a tertiary alkanethiolate.[21] In the crystal structure of a cysteine ethyl ester (CysEtH) complex with silver(I), $Ag_2(CysEt)(NO_3)$, Bell et al. identified two different Ag(I) sites, one strongly coordinated to thiolate groups forming −Ag−S(R)−Ag−S(R)− zigzag chains and the other bound to both thiolate and amine groups.[27] However, the crystal structures of Ag(HPen) and $Ag_2(CysEt)(NO_3)$ were not described in detail, nor were they deposited in the CSD. On the basis of X-ray powder diffraction patterns, Bell et al. suggested layered structures for microcrystalline Ag(I)−cysteine and Ag(I)−glutathione complexes prepared in acetonitrile containing 2% triethylamine,[27,28] as proposed by Dance et al. for silver(I) complexes of primary alkane- and arenethiolates.[20] However, no further structural information such as bond distances or bond angles was provided. Syntheses of the solid silver(I) glutathione compounds $Ag(H_2Glu)$, $Ag_2(HGlu)$, $Ag_3(Glu)$, and $Ag_2(H_2Glu)ClO_4$ have been reported, where the authors suggest on the basis of acid dissociation constants that Ag(I) coordination occurs via −S and/or deprotonated amine sites.[29] Complexes formed between silver(I) and glutathione were also examined using solid-state IR, elemental, and thermal analyses by Ahmad et al., who reported the formation of a 1/1 Ag(I)−glutathione compound.[30] Recently, Costa et al. used DFT calculations and solid-state ^{13}C NMR and IR spectroscopy to suggest that in the compound $Ag(HPen)\cdot H_2O$, obtained at pH 5.0, the Ag(I) ions are surrounded by four bridging thiolate groups.[31] Ag(I)−thiolate (1/1) complexes with antimicrobial activity formed with *N*-acetylmethionine and *N*-acetylcysteine have been investigated with X-ray crystallography and ^{109}Ag and ^{13}C NMR spectroscopy.[32,33]

At very low thiolate concentrations, $[RS^-]_{tot} < 10^{-6}$ mol dm^{-3} (at the "mononuclear wall"), $[Ag_2SR]^+$, $[AgSR]$, and $[Ag(SR)_2]^-$ complexes are proposed to form in aqueous solution at pH 1−2, while at higher thiolate concentrations chainlike polynuclear silver(I) species would persist in the form of $[Ag\{S(R)Ag\}_n]^+$ cations in an excess of Ag^+, or as $[S(R)\{AgS(R)\}_n]^-$ anions for $[RS^-] > [Ag^+]$. At $[RS^-]_{tot} > 10^{-3.2}$ mol dm^{-3}, these species condense ($n \rightarrow \infty$) and precipitate.[34] Polynuclear silver(I) cysteine and glutathione species have been reported for dilute solutions, 8 mmol dm^{-3} $AgNO_3$ and 10 mmol dm^{-3} cysteine (pH 9.85) or glutathione (pH 8.0), with cysteine binding to the Ag(I) ions through its thiolate and amino groups and glutathione only through its thiolate group.[35] An apparent formation constant ($K'_f = 3.2 \times 10^{-13}$) was ascribed to the complex $[Ag(Cys)_2]^{3-}$ from a potentiometric study.[36] Later, Adams and Kramer with the same method estimated conditional formation constants for mononuclear 1/1 and 1/2 complexes for silver(I) cysteine (log $\beta'_1 = 11.9 \pm 0.49$ and log $\beta'_2 = 15.2 \pm 0.39$) and glutathione (log $\beta'_1 = 12.3 \pm 0.32$ and log $\beta'_2 = 14.3 \pm 0.79$),[37] respectively, concluding that coordination only occurs via the thiol groups in the pH range 4−8. Recently, Alekseev et al. reported formation constants (log β) for several Ag(I)−cysteine complexes: $AgCys^-$ (11.14 ± 0.10), AgHCys (20.77 ± 0.06), Ag_2Cys (20.32 ± 0.17), and Ag_2HCys^+ (27.28 ± 0.12).[38]

The present investigation was performed to increase the general understanding of silver(I) complex formation with biologically relevant thiol-containing ligands, including cysteine, penicillamine, and glutathione, as part of our systematic studies on heavy-metal complex formation with such ligands in aqueous solution and in the solid state.[39−45] We report crystal structures of the compounds $(NH_4)Ag_2(HCys)(Cys)\cdot H_2O$ (**1**) and $Ag(HPen)\cdot H_2O$ (**2**), from crystals prepared at pH ∼10 for both compounds. The latter crystal structure is very similar to that described for Ag(HPen) by Bell and co-workers;[27] the compound is probably the same, although more detailed structural information is provided here. We have used combinations of EXAFS and ^{109}Ag NMR spectroscopic techniques to study the Ag(I) complex formation with cysteine (pH ∼10−11), penicillamine (pH ∼9.0), and glutathione (pH ∼11.0) in alkaline aqueous solution. To the best of our knowledge, this is the first report on the structure of Ag(I)−-glutathione complexes in a 1/2 mole ratio, providing the average Ag−S bond distance.

^{109}Ag NMR spectroscopy is a potentially useful tool for investigating the coordination environment of the Ag(I) ion. The two stable silver isotopes ^{107}Ag and ^{109}Ag with natural abundances 51.8% and 48.2%, respectively, both have nuclear spin $I = {}^1/_2$. Despite its lower natural abundance, ^{109}Ag is normally preferred for NMR studies because of its slightly higher sensitivity. Difficulties in obtaining ^{109}Ag NMR spectra with good *S*/*N* ratio are due to the extremely long spin−lattice relaxation time (T_1) and relatively low sensitivity (receptivity) of the ^{109}Ag nucleus, which is 4.94×10^{-5} relative to ^1H and

dx.doi.org/10.1021/ic400192c | Inorg. Chem. 2013, 52, 4593−4602

0.290 relative to ^{13}C.[46−49] The ^{109}Ag chemical shift is affected by several factors, including the type and number of coordinating atoms, the number of bridging vs terminal donor atoms (e.g., thiolates), bond distances and bond angles, the solvent and the nature of the counterion, and also the concentration.[47,49−53] For example, the ^{109}Ag chemical shift differs ∼50 ppm for 1 and 9 mol dm^{-3} (nearly saturated) $AgNO_3$ aqueous solutions.[47,48] Solid silver(I) acetate[54] and $AgNO_3$ in aqueous solution have frequently been used as references for calibrating ^{109}Ag NMR chemical shifts; however, often the $AgNO_3$ concentration is not stated, which makes direct comparisons of ^{109}Ag NMR chemical shifts reported by different groups difficult.[48,49]

EXPERIMENTAL SECTION

Sample Preparation. All samples were synthesized and handled under an argon atmosphere using O_2-free water, prepared by boiling and bubbling argon through when cooling. Silver(I) perchlorate hydrate, L-cysteine, D-penicillamine, glutathione, ammonia, and sodium hydroxide were used as received from Sigma Aldrich. During the syntheses the pH was monitored with a Corning Semi-Micro electrode.

Silver(I) Cysteine/Penicillamine and Glutathione Solutions. Table 2 provides the composition of the series of alkaline silver(I) solutions with cysteine (A−E, P), penicillamine (F−J, Q), and glutathione (K−O), for ligand-to-metal mole ratios L/Ag = 2−10 and pH 9−11. Solutions A−J containing $C_{Ag} \approx 80-100$ mmol dm^{-3} were prepared for EXAFS measurements by adding $AgClO_4 \cdot H_2O$ (1−1.5 mmol) to aqueous solutions of cysteine or penicillamine (3−15 mmol) in O_2-free water, which resulted in a drop in pH from 4.3−4.8 to 1.6−2.9 and immediate precipitation. Sodium hydroxide solution (6 mol dm^{-3}) was added dropwise until the precipitate dissolved. The total volume was adjusted, depending on the initial amount of Ag(I) perchlorate, to 10.0 or 15.0 mL for solutions A−D and F−I and reached 17.6−17.7 mL for solutions E and J. The total Ag(I) concentration $C_{Ag(I)}$ was confirmed with a Thermo Jarrell Ash AtomScan 16 inductively coupled plasma atomic emission spectrophotometer (ICP-AES). Solution P was prepared by mixing 9.2 mmol of $AgClO_4 \cdot H_2O$ and 20 mmol of cysteine (total volume 11.4 mL); for solution Q containing 5 mmol of $AgClO_4 \cdot H_2O$ and 10 mmol of penicillamine the total volume was adjusted to 10.0 mL.

A similar procedure was followed for the series of Ag(I)−glutathione solutions K−O (Table 2). Glutathione (0.26−1.3 mmol) was dissolved in O_2-free water and $AgClO_4 \cdot H_2O$ (0.13 mmol) added to the solution. A precipitate formed at pH ∼2.2−2.4, which dissolved at pH ∼11. The total volume (12.4−12.8 mL) was recorded in each case. Due to the low solubility of glutathione, the total Ag(I) concentration in solutions K−O was kept at $C_{Ag(I)} \approx 0.01$ mol dm^{-3}.

For ^{109}Ag NMR spectroscopy measurements, two concentrated Ag(I) solutions ($C_{Ag} \approx 0.8$ and 0.5 mol dm^{-3}, L/Ag mole ratio ∼2) were prepared with cysteine (P) and penicillamine (Q), respectively. Cysteine (20 mmol) was dissolved in O_2-free water and spiked with 1 mL of O_2-free D_2O. When $AgClO_4 \cdot H_2O$ (9.2 mmol) was added, a yellow precipitate immediately formed (pH 0.5). Sodium hydroxide (10 mol dm^{-3}) was added dropwise until the precipitate dissolved (pH 10.9). Similarly, adding 5 mmol of $AgClO_4 \cdot H_2O$ to a penicillamine solution (10 mmol) in O_2-free water + D_2O immediately formed a light yellow precipitate (pH 0.4), which dissolved at pH 9.4.

Crystalline Compounds $(NH_4)Ag_2(HCys)(Cys) \cdot H_2O$ (1) and $Ag(HPen) \cdot H_2O$ (2). Cysteine or penicillamine (1.0 mmol) was dissolved in 3 mL of a 5/1 methanol/water mixture. $AgClO_4 \cdot H_2O$ (1.0 mmol) was added, and a precipitate immediately formed. Ammonia was added until the precipitate dissolved (pH ∼10). Both solutions were kept covered with aluminum foil at room temperature. Thin, platelike crystals of **1** formed after 2 days, while needle-shaped crystals of **2** were isolated after slowly evaporating the solvent over 7 days.

X-ray Crystallography. Crystals of **1** and **2** were coated with Paratone 8277 oil (Exxon) and mounted on a glass fiber. Data collection was performed with a Nonius Kappa CCD diffractometer using a combination of ϕ and ω scans.[55] The data were corrected for Lorentz and polarization effects and for absorption using the multiscan method.[56] Details of crystal structure data collection and refinements are provided in Table 3. The structures were solved by direct methods[57] and expanded using Fourier techniques.[58] For **1**, hydrogen atoms were included in the refinements using a riding model keeping O−H = 0.82 Å, N−H = 0.92 Å (for NH_2) or 0.91 Å (for -NH_3^+/NH_4^+), and C−H = 0.96 Å. For **2** the hydrogen atoms, positioned at geometrically idealized positions, were not refined. The methyl H atoms were described as disordered over six sites. Full-matrix least-

Table 2. Composition of Ag(I) Solutions with Cysteine, Penicillamine, and Glutathione[a,b]

ligand (L)	solution	L/Ag ratio	$C_{Ag(I)}$	C_L	pH
cysteine	A	2.0	100	200	11.0
	B	3.0	100	300	10.3
	C	4.0	100	401	10.1
	D	5.0	100	500	10.0
	E	10.1	84	848	11.0
	P	2.2	807	1754	10.9
penicillamine	F	2.0	100	200	9.0
	G	3.0	100	300	9.0
	H	4.0	100	400	9.0
	I	5.0	100	496	9.0
	J	10.0	88	877	9.0
	Q	2.0	500	1000	9.4
glutathione	K	2.0	10.4	21.0	10.9
	L	3.0	10.2	30.7	11.1
	M	4.0	10.1	40.6	11.0
	N	5.0	10.2	51.2	11.2
	O	10.0	10.2	102.4	11.0

[a]Concentrations C in mmol dm^{-3}. [b]ICP analysis for cysteine and penicillamine solutions verified $C_{Ag(I)}$ within ±5 mmol dm^{-3}.

Table 3. Crystal Data and Structure Refinement Details for the Ag(I) Crystals 1 and 2[a]

	$(NH_4)Ag_2(HCys)(Cys) \cdot H_2O$ (1)	$Ag(HPen) \cdot H_2O$ (2)
chem formula	$C_6H_{17}Ag_2N_3O_5S_2$	$8 \cdot C_5H_{12}AgNO_3S$
formula wt (g/mol)	491.08	2192.72
space group	$P2_1$ (No. 5)	$P1$ (No. 1)
a (Å)	9.163(3)	11.632(3)
b (Å)	4.794(3)	12.699(4)
c (Å)	16.105(10)	13.603(5)
α (deg)	90	95.315(14)
β (deg)	105.35(4)	104.618(19)
γ (deg)	90	113.660(18)
V (Å^3)	682.2(6)	1737.7(10)
Z	2	1
D_{calcd} (g/cm^3)	2.391	2.095
T (K)	173(2)	173(2)
λ (Å)	0.71073 (Mo Kα)	0.71073 (Mo Kα)
μ (mm^{-1})	3.191	2.520
F(000)	480	1088
θ range (deg)	3.00 −27.49	3.12 −27.53
R1, wR2 ($I \geq 2\sigma(I)$)	0.0325, 0.0753	0.0619, 0.0969

[a]$R1 = \sum|F_o - F_c|/\sum|F_o|$; $wR2 = [\sum w(F_o^2 - F_c^2)^2/\sum w(F_o^2)^2]^{1/2}$.

dx.doi.org/10.1021/ic400192c | Inorg. Chem. 2013, 52, 4593−4602

squares refinements were performed using SHELXL97,[59] with essentially featureless final difference Fourier maps.

^{109}Ag NMR Spectroscopy. The ^{109}Ag NMR spectra were collected with a Bruker AMX-300 spectrophotometer with a base frequency of 13.963 MHz. ^{109}Ag and ^{39}K are NMR nuclei with closely adjacent resonance frequencies (^{39}K 14.006 MHz), but their relaxation times (T_1) are quite different: 60−950 s for ^{109}Ag but only 2×10^{-2} s for ^{39}K.[60] Therefore, initially a 90° pulse ^{39}K NMR signal was calibrated for a saturated KBr solution in D_2O. Then the value was transferred to the ^{109}Ag NMR signal for a 1.0 mol dm^{-3} solution of silver nitrate in D_2O, which was set as reference (0 ppm). The ^{109}Ag NMR spectra were recorded using a 30° pulse program, with a sweep width of −150 to +1250 ppm. All spectra were measured with a 10 mm broad band (BBO) probe and a 100 s delay at 300 K. In all, 188 and 664 scans were collected for solutions P and Q, respectively.

EXAFS Spectroscopy. The Ag K-edge X-ray absorption spectra of Ag(I)−cysteine and Ag(I)−penicillamine solutions with [Ag$^+$] ≈ 80−100 mmol dm^{-3} were measured at beamline 10-B at the Photon Factory of the High Energy Accelerator Research Organization in Tsukuba, Japan. The operating conditions were 2.5 GeV with ring currents between 250 and 300 mA. A fully tuned Si(311) channel-cut monochromator crystal was used for which the second order harmonic is forbidden, i.e. radiation with twice the energy can be neglected, and also the intensity of the third harmonic is negligible because of the steep falloff of the synchrotron radiation spectrum at higher energies.[61] The solution samples were held in 10 mm Teflon spacers with 5 μm polypropylene film windows. The spectra were measured in transmission mode with argon in the first ion chamber (I_0, before the sample) and krypton in the second (I_1), collecting three scans for each sample. The energy scale was externally calibrated using an Ag foil, setting the first inflection point at 25514.0 eV.

The Ag K-edge X-ray absorption spectra for Ag(I)−glutathione solutions containing $C_{Ag(I)}$ ≈ 10 mM were collected at BL 2-3 at the Stanford Synchrotron Radiation Lightsource (SSRL) under dedicated conditions of 3.0 GeV and 70−100 mA. Higher harmonics were rejected by detuning the Si(220) double crystal monochromator to 50% of the maximum incident beam intensity at the end of the scan. For these solutions 10−16 scans were measured in fluorescence mode using a 13-element Ge detector. The energy scale was internally calibrated by means of a silver foil placed between the second (I_1) and third (I_2) ion chambers, which were filled with krypton.

Ag K-edge X-ray absorption spectra of the highly concentrated Ag(I)−cysteine (L/Ag = 2.2, $C_{Ag(I)}$ = 807 mmol dm^{-3}) and Ag(I)−penicillamine solutions (L/Ag = 2.0, $C_{Ag(I)}$ = 500 mmol dm^{-3}) intended for ^{109}Ag NMR were also collected under similar conditions at the BL 2-3 at the SSRL facility, with 4 and 9 scans in transmission mode, respectively, using 3 mm Teflon spacers.

EXAFS Data Analysis. For every Ag K-edge X-ray absorption spectrum measured in fluorescence mode, the I_f/I_0 ratios for each channel of the Ge detector were checked and compared for all scans before averaging, using the EXAFSPAK suite of programs.[62] For the spectra measured in transmission mode, the log (I_1/I_0) values were averaged for overlapping scans. The EXAFS oscillation was extracted using the WinXAS 3.1 program,[63] by subtracting a first-order polynomial background from the pre-edge region, followed by normalization over the edge step. The energy scale was converted into k space, where $k = [(8\pi^2 m_e/h^2)(E - E_0)]^{1/2}$, using a threshold energy of E_0 = 25514.0−25515.0 eV. A seven-segment spline was used to remove the atomic background contribution in the post-edge region. EXAFS model functions, $\chi(k)$, were computed using the FEFF 8.1 program.[64,65] Atomic coordinates from the crystal structure of $(NH_4)Ag_2(HCys)(Cys)\cdot H_2O$ (**1**) were used as input to calculate the amplitude function, phase shift, and mean free path parameters. Least-squares curve fitting of the model functions to the k^3-weighted experimental EXAFS spectra over the k range 2.5−15.0 Å^{-1} were used to refine the structural parameters, allowing the bond distance (R), Debye−Waller parameter (σ^2), and ΔE_0 (one value common for all scattering paths) to float, while keeping the amplitude reduction factor (S_0^2) and sometimes the coordination number (N) fixed.

RESULTS AND DISCUSSION

Crystal Structures of $(NH_4)Ag_2(HCys)Ag(Cys)\cdot H_2O$ (1) and $Ag(HPen)\cdot H_2O$ (2). The crystal structure of **1** consists of Ag−thiolate layers parallel to the *ab* plane of the unit cell, which are held together by hydrogen bonding to water molecules (O5) and ammonium ions (N3) (Figure 1 and Figure S-1 (Supporting Information)). Within the layers there are two types of silver(I) coordination environments: pseudotetrahedral AgS_3N and nearly planar trigonal AgS_3. The silver ion of the AgS_3N site, Ag(1), coordinates three thiolate sulfur atoms S(1) from cysteinate (Cys^{2-}) ligands. The short Ag−N(1) bond distance, 2.306(5) Å, indicates a strong bond (cf. Table 1), while the Ag−S(1)^{i} bond, 2.802(2) Å, to this chelating Cys^{2-} ligand is weaker than the bridging ones, Ag−S(1)^{ii} = 2.515(2) Å and Ag−S(1) = 2.657(2) Å (Table 4). Thus, each S(1) atom connects three Ag(1) sites in a double chain running parallel to the *b* axis (see Figure 1 (left) and Figure S-1).

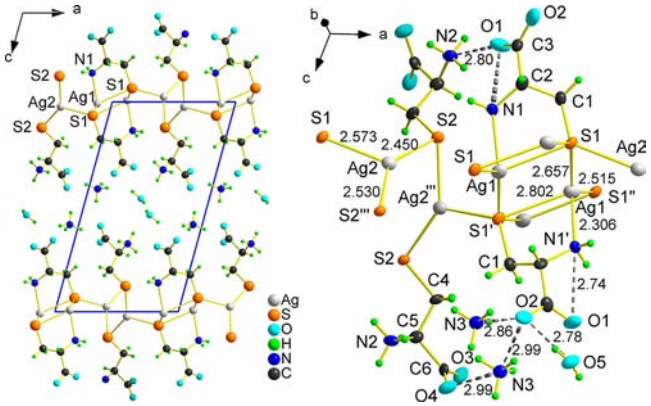

Figure 1. (Left) In the Ag(I)−cysteinate compound $(NH_4)Ag_2(HCys)Ag(Cys)\cdot H_2O$ (**1**) layers of Ag−thiolates with AgS_3N (Ag1) and AgS_3 (Ag2) coordination in the *ab* plane of the unit cells are connected via hydrogen bonds that are shown as dashes (right) from carboxylate oxygen to water molecules (O5) and ammonium ions (N3). Thermal ellipsoids (right) are shown with 70% probability, and bond distances are given in Å.

Two thiolate sulfur atoms from $HCys^-$ ligands, S(2), connect the Ag(2) atoms with the bond distances Ag(2)−S(2) = 2.450(2) Å and Ag(2)−S(2)^{iii} = 2.530(2) Å, forming a single-bridged chain with relatively short Ag(2)···Ag(2) distances of 2.928(1) Å (Figure 1). Each S(1) atom of the cysteinate Cys^{2-} ligand also forms a bond to the silver ion Ag(2) with the Ag(2)−S(1) bond distance of 2.573(2) Å. The chains of single-bridged AgS_3 entities are thus directly connected to the AgS_3N double chains (Figure S-1), giving rise to the Ag−thiolate layer. The average Ag−S bond distance in the trigonal AgS_3 entities is 2.518 Å, which is within the range typically found for Ag(I)−thiolate complexes with AgS_3 coordination (Table 1). The deprotonated carboxylate group C(3) of the cysteinate (Cys^{2-}) ligand has the C−O bond distances C−O(1) = 1.232(8) Å and C−O(2) = 1.267(8) Å; the latter is prolonged due to strong hydrogen bonding to the water molecule (O5) and the ammonium NH_4^+ ion (N3) (Figure 1 (left)). Also, the carboxylate group of the $HCys^-$ ligand is deprotonated with the C−O bond distances 1.241(8) and 1.255(9) Å, while the amino group is protonated. Selected interatomic distances and angles are presented in Table 4.

dx.doi.org/10.1021/ic400192c | Inorg. Chem. 2013, 52, 4593−4602

Table 4. Selected Interatomic Distances and Angles for 1 and 2[a]

$(NH_4)Ag_2(HCys)Ag(Cys)\cdot H_2O$ (**1**)			
Ag(1)–N(1)^{i}	2.306(5)	Ag(2)–S(1)	2.573(2)
Ag(1)–S(1)^{ii}	2.515(2)	Ag(2)–S(2)	2.450(2)
Ag(1)–S(1)	2.657(2)	Ag(2)–S(2)^{iii}	2.530(2)
Ag(1)–S(1)^{i}	2.802(2)	Ag(2)–Ag(2)^{iii}	2.928(1)
N(1)^{i}–Ag(1)–S(1)	100.11(16)	S(1)^{i}–Ag(1)–S(1)^{ii}	107.32(6)
N(1)^{i}–Ag(1)–S(1)^{i}	76.26(13)	S(1)–Ag(2)–S(2)	122.00(6)
N(1)^{i}–Ag(1)–S(1)^{ii}	117.30(16)	S(1)–Ag(2)–S(2)^{iii}	97.48(6)
S(1)–Ag(1)–S(1)^{i}	103.43(6)	S(2)–Ag(2)–S(2)^{iii}	140.37(4)
S(1)–Ag(1)–S(1)^{ii}	135.89(7)	Ag(2)–S(2)–Ag(2)^{iii}	71.99(6)
$Ag(HPen)\cdot H_2O$ (**2**)			
Ag(1)–S(1)	2.360(3)	Ag(5)–S(5)	2.356(3)
Ag(1)–S(2)^{iv}	2.356(4)	Ag(5)–S(6)^{iv}	2.369(3)
Ag(2)–S(2)	2.416(3)	Ag(6)–S(6)	2.426(3)
Ag(2)–S(3)	2.401(3)	Ag(6)–S(7)	2.394(3)
Ag(3)–S(3)	2.411(4)	Ag(7)–S(1)	2.415(3)
Ag(3)–S(4)	2.382(3)	Ag(7)–S(8)	2.387(3)
Ag(4)–S(4)	2.394(3)	Ag(8)–S(7)	2.376(3)
Ag(4)–S(5)	2.417(3)	Ag(8)–S(8)	2.376(3)
S(1)–Ag(1)–S(2)^{iv}	176.63(12)	S(5)–Ag(5)–S(6)^{iv}	175.25(12)
S(2)–Ag(2)–S(3)	172.04(12)	S(6)–Ag(6)–S(7)	167.50(11)
S(3)–Ag(3)–S(4)	161.78(12)	S(1)–Ag(7)–S(8)	172.53(11)
S(4)–Ag(4)–S(5)	172.11(12)	S(7)–Ag(8)–S(8)	173.45(13)

[a]Symmetry transformations used to generate equivalent atoms are as follows. For **1**: (i) $2-x, y-{}^1/_2, -z$; (ii) $x, y-1, z$; (iii) $1-x, y+{}^1/_2, -z$. For **2**: (iv) $x-1, y, z$.

The double-helical chain structure of $Ag(HPen)\cdot H_2O$ (**2**) was described by Bell et al. in 1997;[27] however, unit cell dimensions and atomic coordinates were not provided, nor was the CIF file deposited in the CSD. As described previously, the most prominent feature is the two intertwined polymeric $\{-Ag-(SR)-\}_n$ strands containing nearly linear AgS_2 units (Figure 2 and Figure S-2 (Supporting Information)). The

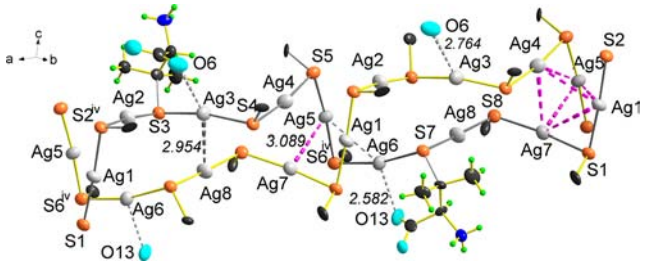

Figure 2. In the crystal structure of $Ag(HPen)\cdot H_2O$ (**2**), eight Ag(HPen) monomers connect with nearly linear AgS_2 coordination, forming two intertwined polymeric strands in a double helix along the *a* axis. For clarity only the thiolate sulfur and its nearest carbon atom are shown (except for S3 and S7). Dashed lines indicate the closest Ag···Ag and Ag···O interactions (see text). Thermal ellipsoids are shown with 70% probability, and bond distances are given in Å.

strands, which are formed by bridging thiolate groups from the penicillamine ligands ($HPen^-$), run parallel to the *a* axis and twist jointly at every fourth silver(I) ion in a double helix. The Ag–S bond distances vary from 2.356(4) to 2.426(3) Å (Table 4), within the range expected for Ag(I)–thiolate complexes with near-linear AgS_2 coordination (Table 1). The largest deviations from linearity occur around the Ag(3) and Ag(6) centers with S–Ag–S angles of 161.78(12) and 167.50(11)°, respectively, probably due to weak interactions with nearby carboxylate oxygen: Ag(3)···O(6) = 2.764(8) Å and Ag(6)···O(13) = 2.582(9) Å (Figure 2).

Both structures display short Ag···Ag distances. In $(NH_4)Ag_2(HCys)Ag(Cys)\cdot H_2O$ (**1**), the singly bridged Ag(2)···Ag(2)^{iii} distance at 2.928(1) Å is only slightly longer than the Ag···Ag separation in metallic silver (2.889 Å)[66] and considerably shorter than the sum of the van der Waals radii (3.44 Å).[67]

Within the two polymeric strands of $Ag(HPen)\cdot H_2O$ (**2**), the closest "ligand unsupported" (i.e., nonbridged) contact between neighboring silver ions, Ag(3)···Ag(8) = 2.954(2) Å, is shorter than the shortest thiol-bridged Ag···Ag distance, Ag(5)···Ag(6) = 3.151(3) Å. At the twist in the crossover, the silver ions Ag(1), Ag(4), Ag(5), and Ag(7) form an almost regular tetrahedron, with rather short nonbridged Ag···Ag contacts: Ag(5)···Ag(7) = 3.089(2) and Ag(1)···Ag(4) = 3.255(2) Å. These non-bridged contacts were previously reported as nonbonding while providing structural stabilization.[27] However, a similaly short Ag···Ag contact, 2.954(4) Å, was considered as weakly bonding in an Ag(I) carbene complex,[68] as was also an Ag···Ag interaction of 2.8987(9) Å between two silver ions with AgS_2O_2 coordination in an Ag(I)–acetylmethionine compound.[32] While a short Ag···Ag distance does not necessarily imply bond formation,[21,69] weak interactions can occur between ions with d^{10} electronic configuration even when not supported by bridging ligands[66,70,71] and may influence the physical properties of Ag(I) compounds.[32,72] In the present case, the slight deviations of the S–Ag–S angle from linearity in those AgS_2 entities in close proximity (Figure 2) do not clearly indicate whether the short Ag(3)···Ag(8) and Ag(5)···Ag(7) contacts are repulsive or attractive, since both Ag(3) and Ag(5) are affected by other interactions.

Ag(I)–Thiolate Complexes in Alkaline Aqueous Solution. Structural parameters obtained from least-squares curve fitting of model functions to the k^3-weighted Ag K-edge EXAFS spectra (Figure 3 and Figure S-3 (Supporting Information)) are presented in Table 5. The corresponding Fourier transforms (FT) obtained for alkaline Ag(I) aqueous solutions with cysteine (A–E), penicillamine (F–J), and glutathione (K–O) with L/Ag ratios of 2–10 show a single symmetric Ag–S peak at ~2 Å (not corrected for phase shift).

Silver(I)–Glutathione Solutions. The Ag K-edge EXAFS spectra of the Ag(I)–glutathione aqueous solutions (K–O) containing $C_{Ag(I)}$ = 10 mmol dm^{-3} and L/Ag mole ratios 2.0–10.0 (pH 11) show EXAFS oscillations with similar frequencies (Figure 3 and Figure S-4 (Supporting Information)). The small variations in the mean Ag–S bond distance (2.36–2.38 Å) and the corresponding Debye–Waller parameters (σ^2 = 0.0024–0.0056 $Å^2$) indicate similar coordination in the dominating species for these solutions (Figure 3, Table 5). At high mole ratios (with up to 80 mmol dm^{-3} free Glu^{3-}) the Ag–S bond distances tend to become shorter and the corresponding σ^2 values smaller. These Ag–S distances are slightly shorter than the mean Ag–S distance of 2.39 Å for Ag(I)–thiolate complexes with near-linear AgS_2 coordination (Table 1). Similarly short Ag–S distances are found both for mononuclear (CSD code: HOBWIE),[73] and oligomeric Ag(I) complexes (CSD codes: CAYZUX10, CEPKIR, and FIMFOW)[19,21,22] with bulky thiolate ligands. Only for the L/Ag mole ratios 2.0 and 3.0 (solutions K and L) could an Ag···Ag interaction (~3.0 Å) be included that slightly improved the model fitting (Table 5). It can be concluded that, in solutions K–O, mononuclear

dx.doi.org/10.1021/ic400192c | Inorg. Chem. 2013, 52, 4593–4602

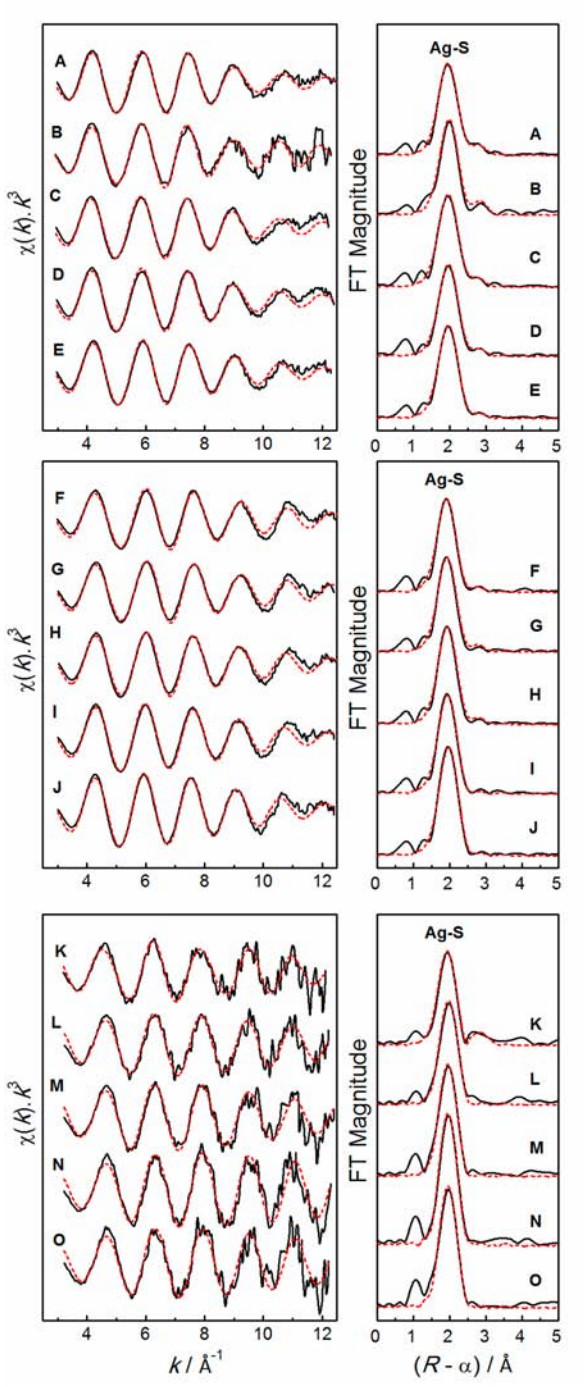

Figure 3. Ag K-edge EXAFS spectra and corresponding Fourier transforms for Ag(I) alkaline aqueous solutions (pH 9–11), containing cysteine (top), penicillamine (middle), and glutathione (bottom) with L/Ag ratios 2–10 (see Table 2). The curve-fitting results (experimental, black solid line; fit, red dashed line) are presented in Table 5 (labeled footnote *c*).

Table 5. Structural Parameters Derived from Ag K-Edge EXAFS Least-Squares Curve Fitting for the Ag^{I}–L (L = Cysteine, Penicillamine, Glutathione) Solutions A–Q at pH 9.0–11.0[a]

solution (L/Ag^{+})	Ag–S			Ag···Ag			
	N	*R* (Å)	σ^2 (Å²)	*N*	*R* (Å)	σ^2 (Å²)	$\mathcal{R}$[b]
			L = Cysteine				
A (2.0)	3.1	2.44	0.0109				21.5
	2.9	2.44	0.0102	1*f*	2.93	0.016	18.1
	3.0	2.44	0.0103	0.5*f*	2.92	0.011	18.0[c]
B (3.0)	2.8	2.46	0.0093				30.0
	2.7	2.46	0.0090	0.5*f*	3.00	0.009	27.7[c]
C (4.0)	3.2	2.45	0.0107				23.8
	3.0	2.45	0.0102	0.5*f*	2.93	0.013	22.2[c]
D (5.0)	3.2	2.45	0.0108				23.2
	3.0	2.45	0.0104	0.5*f*	2.95	0.015	22.5[c]
E (10.1)	3.1	2.45	0.0108				19.3
	3.0	2.45	0.0105	0.5*f*	2.94	0.018	18.9[c]
P (2.2)	2.4	2.47	0.0085				21.1
	2.3	2.47	0.0081	0.5*f*	2.93	0.014	19.5[c]
			L = Penicillamine				
F (2.0)	2.4	2.39	0.0084				22.3
	2.3	2.40	0.0084	0.5*f*	2.91	0.019	22.5[c]
G (3.0)	2.4	2.40	0.0084				21.4
	2.3	2.40	0.0082	0.5*f*	2.91	0.016	21.0[c]
H (4.0)	2.6	2.41	0.0088				20.8
	2.5	2.41	0.0086	0.5*f*	2.91	0.017	20.7[c]
I (5.0)	2.8	2.42	0.0094				21.9
	2.8	2.42	0.0093	0.5*f*	2.80	0.029	21.6[c]
J (10.0)	3.1	2.44	0.0094				20.9
	3.1	2.44	0.0093	0.3*f*	2.85	0.022	20.8[c]
Q (2.0)	1.8	2.40	0.0072				20.8[c]
			L = Glutathione				
K (2.0)	1.6	2.37	0.0054				39.8
	1.6	2.37	0.0057	0.5*f*	2.98	0.009	38.9[c]
L (3.0)	1.5	2.38	0.0045				39.1[c]
	1.6	2.38	0.0047	0.5*f*	3.02	0.010	38.8
M (4.0)	1.7	2.37	0.0047				35.0[c]
N (5.0)	1.5	2.36	0.0024				35.8[c]
O (10.0)	1.5	2.36	0.0034				42.4[c]

[a]See Figure 3, Figure S-3 (Supporting Information), and Table 2. Fitting *k* range 3.0–12.5 $Å^{-1}$; $S_0^2 = 0.9f$ (*f* = fixed); estimated error limits *N* ±20%, *R* ±0.02 Å, σ^2 ±0.001 Å². [b]Residual. [c]Fitted models shown in Figure 3.

$[Ag(Glu)_2]^{5-}$ species with near-linear AgS_2 coordination and strong Ag–S bonds dominate. Possibly a minor amount of oligomeric Ag(I)–glutathione species can aggregate at low mole ratios with Ag···Ag distances around 3.0 Å that only slightly affect the strongly bonded AgS_2 entities.

Silver(I)–Cysteine Solutions. For the Ag(I)–cysteine solutions A–E containing $C_{Ag(I)} \approx 80–100$ mmol dm^{-3}, the EXAFS oscillations and also their FT peaks overlap (Figure S-4, top (Supporting Information)). The narrow ranges for the refined Ag–S coordination number, ~ 2.7–3.0, and the mean Ag–S bond distance, 2.44–2.46 Å, show that the increase in cysteinate concentration did not significantly influence the Ag(I) speciation. This range for the mean Ag–S distance is considerably longer than that obtained for Ag(I)–glutathione solutions (2.36–2.38 Å), attributed to mononuclear $[Ag(Glu)_2]^{5-}$ species with near-linear AgS_2 coordination (see above). Relatively high values of the Debye–Waller parameter (σ^2) for the Ag–S scattering path for solutions A–E (Table 5) signify that, in addition to thermal movements, there are large variations in the Ag–S bond distances, which are between the average values for crystalline Ag(I)–thiolate complexes with near-linear AgS_2 coordination (2.39 Å) and trigonal AgS_3 coordination (2.51 Å), and are also comparable with the average mean distances in Ag(I)–thiolate complexes with

dx.doi.org/10.1021/ic400192c | Inorg. Chem. 2013, 52, 4593–4602

AgS_2N coordination, Ag−S = 2.49 Å and Ag−N = 2.29 Å (Table 1). Similar mean Ag−S bond distances (2.44−2.45 Å) were obtained from the S K-edge EXAFS spectra of rabbit liver Ag(I) metallothionein ($Ag_{12}MT$ and $Ag_{17}MT$) and then proposed to correspond to digonal AgS_2 coordination with some bridging *S*-thiolates.[74]

Including the Ag···Ag scattering path in the fitted models improved the fitting, and the interatomic distance consistently refined to 2.92−3.00 Å (Table 5), similar to the singly bridged Ag(2)···Ag(2)^{iii} distance of 2.928(1) Å in the chain of trigonal AgS_3 entities in **1** (Table 4), which there corresponds to a quite acute Ag−S−Ag angle of 71.99(6)°. However, the contribution of this scattering path was often diffuse due to its high Debye−Waller parameter. When the number of Ag···Ag interactions are kept fixed to 1.0 (as in a polymeric chain), their σ^2 parameters raised to quite high values. For solutions with L/Ag mole ratios ≥3 the number was set to 0.5, which would correspond to a mix of mononuclear and oligomeric complexes with a range of Ag···Ag distances around the refined values, 2.9−3.0 Å. One motivation for proposing oligomeric, singly bridged complexes with AgS_3 coordination and short Ag···Ag distances in the Ag(I)−cysteine solutions A−E is that species similar to fragments of the polymeric structure **1** could be present that are held together by intramolecular hydrogen bonding between the ligands and possibly also stabilized by hydrophobic interactions between the Ag atoms in trigonal AgS_3 units.

Considering possible Ag(I)−amine coordination as in the structure of **1**, an AgS_2N model was used for fitting the EXAFS spectrum of solution A with mole ratio L/Ag = 2.0, resulting in a fitting residual similar to that for the AgS_3 model (see Table S-2 (Supporting Information)). The average Ag−S and Ag−N distances obtained, 2.45 ± 0.02 and 2.32 ± 0.02 Å, respectively, are comparable with corresponding mean distances in Ag(I)−thiolate complexes with AgS_2N coordination (Table 1). Since the EXAFS spectra of solutions A−E overlap, the AgS_2N model is expected to fit well also for other Ag(I)−cysteine solutions.

To find the preferable model (AgS_3 or AgS_2N) for describing the Ag(I)−cysteine coordination in solutions A−E, a concentrated solution P, with $C_{Ag(I)}$ = 0.8 mol dm^{-3} and cysteine/Ag(I) mole ratio 2.2, was prepared. The ^{109}Ag NMR spectrum of this solution showed a chemical shift at 1103.1 ppm (Figure 4), which is comparable to those attributed to AgS_3 coordination sites (1000−1250 ppm) in yeast Ag(I)−metallothionein (Ag_8MT), both referenced relative to 1.0 mol dm^{-3} $AgNO_3$ solution (0.0 ppm).[52,75] For the structurally characterized crystalline compounds $AgS(CH_2)_3CH_3$ and $[Ph_4P]_2[Ag_4(SCH_2C_6H_4CH_2S)_3]\cdot 6CH_3OH$ with AgS_3 coordination, solid-state ^{109}Ag NMR isotropic chemical shifts in the range δ_{iso} 952−1230 ppm have been reported.[76,77] The reference was an $AgNO_3$ aqueous solution with unknown concentration (0.0 ppm), with silver acetate used as a secondary reference set to 382.7 and 401.2 ppm.[54] Note that there is a ∼50 ppm difference between $\delta(^{109}Ag)$ for 1 and 9 mol dm^{-3} $AgNO_3$ aqueous solution.[47,48]

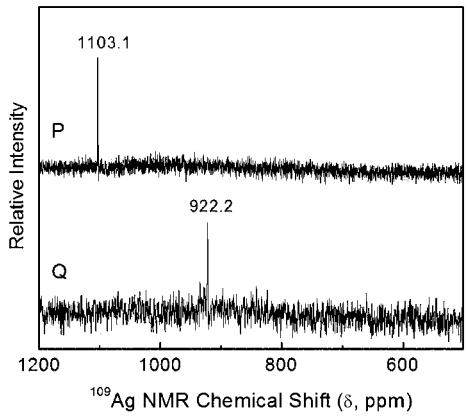

Figure 4. ^{109}Ag NMR spectra of concentrated Ag(I) aqueous solutions with L/Ag ratio ∼2 for cysteine (P) and penicillamine (Q); see Table 2.

EXAFS curve fitting for solution P resulted in a mean Ag−S distance of 2.47 ± 0.02 Å (Table 5, Figure S-3 (Supporting Information)), slightly longer than that of solution A (2.44 ± 0.02 Å), even though the EXAFS oscillations of these two solutions appear rather similar (Figure S-5 (Supporting Information)). Fitting the EXAFS spectrum of solution P with an AgS_2N model resulted in a similar residual (Table S-2 (Supporting Information)); however, this model is not consistent with the chemical shift $\delta(^{109}Ag)$ 1103.1 ppm, indicating mainly AgS_3 coordination (see above). In analogy with solution P, the Ag(I)−cysteine solutions A−E should be dominated by species with AgS_3 coordination. The mean Ag−S bond distance of 2.47 ± 0.02 Å obtained for solution P appears somewhat shorter than the average crystallographic Ag−S distance for the trigonal AgS_3 sites in **1** (2.518 Å) and in Ag(I)−thiolates in CSD (2.51 Å; Table 1). However, it should be noted that shorter Ag−S distances have higher contribution to the overall EXAFS oscillation. For example, the average crystallographic Cd−S bond distances for $[Cd(thiourea)_4](NO_3)_2$ is 2.560 Å, while the mean Cd−S bond length from Cd K-edge EXAFS spectroscopy is 2.53 ± 0.02 Å.[78]

Silver(I)−Penicillamine Solutions. For the alkaline aqueous solution F with $C_{Ag(I)}$ = 0.1 mol dm^{-3} and the penicillamine/Ag(I) mole ratio 2.0, Ag K-edge EXAFS curve fitting resulted in an average Ag−S bond distance of 2.40 ± 0.02 Å (Table 5), which is comparable with the mean Ag−S distance (2.390 Å) for digonal AgS_2 coordination in crystalline $Ag(HPen)\cdot H_2O$ (**2**). A similar average Ag−S distance (2.40 ± 0.02 Å) was obtained for the concentrated solution Q ($C_{Ag(I)}$ = 0.5 mol dm^{-3}) with the same L/Ag mole ratio 2.0 (see Table 5 and Figure S-3 (Supporting Information)). EXAFS curve fitting for both solutions F and Q using an AgS_2N model also resulted in reasonable distances and residuals similar to those of the model including only the Ag−S scattering path (Table S-2 (Supporting Information)). However, for solution Q the ^{109}Ag NMR signal recorded at 922.2 ppm (Figure 4) can be compared with those obtained for AgS_2 sites (790−890 ppm) in yeast Ag(I)−metallothionein (Ag_8MT).[52,75] For the structurally characterized compound $Ag_5L_3(LH)_3(ClO_4)_2$ (L = $S(CH_2)_3N(CH_3)_2$), the solid-state ^{109}Ag NMR isotropic chemical shifts 826 and 1228 ppm were reported for its AgS_2 and AgS_3 coordination sites, respectively (referenced relative to silver acetate).[76,79] For a thiosalicylato−silver(I) complex, the ^{109}Ag NMR chemical shift of 855.6 ppm referenced relative to a saturated $AgNO_3/D_2O$ solution (904.4 ppm when recalibrated relative to 1.0 mol dm^{-3} $AgNO_3$)[49] has been assigned to AgS_2 polymeric species.[80] Similarly, the sodium salt of an Ag(I) complex with trianionic thiomalate showed a ^{109}Ag NMR chemical shift of 868.7 ppm, referenced relative to a saturated $AgNO_3/D_2O$ solution (917.5 ppm when recalibrated relative to 1.0 M $AgNO_3$),[49] which was assigned to AgS_2 coordination within an oligomeric complex.[81] Therefore, Ag(I)−penicill-

dx.doi.org/10.1021/ic400192c | Inorg. Chem. 2013, 52, 4593−4602

amine species with AgS_2 coordination and a mean Ag−S distance of 2.40 ± 0.02 Å dominate, both in solutions F and Q. Including an Ag···Ag scattering path in the fitting model had little influence in improving the EXAFS fitting residuals for these solutions (Table 5).

The EXAFS spectra and corresponding Fourier transforms for the Ag(I)−penicillamine solutions F−J (pH 9.0) are compared in Figure S-4 (Supporting Information). As the total ligand concentration increases from C_{H_2Pen} = 0.2 to 1.0 mol dm^{-3} (L/Ag mole ratios from 2 to 10), the refined mean Ag−S distance increases from 2.40 to 2.44 ± 0.02 Å and the coordination number increases gradually from 2.3 to 3.1 (Table 5), indicating partial formation of Ag(I)−penicillamine complexes with AgS_3 coordination. The formation of trithiolate complexes is evidently much less promoted in an excess of the ligand penicillamine than with cysteine, and significant amounts of the AgS_3 coordinated species only occur for a high excess of penicillamine in alkaline solution. Digonal AgS_2 coordination is also found in the crystal structure of $Ag(HPen)\cdot H_2O$, in contrast to the suggestion from a DFT calculation that the Ag(I) ions are surrounded by four bridging thiolate groups in this compound.[31]

CONCLUSIONS

The Ag(I) complexes with cysteine and penicillamine in the crystal structures of $(NH_4)Ag_2(HCys)Ag(Cys)\cdot H_2O$ (**1**) and $Ag(HPen)\cdot H_2O$ (**2**) with L/Ag mole ratios 1/1 exemplify the flexibility of the silver(I) coordination environment with thiolate ligands. In **1**, layers were formed with mixed AgS_3 and AgS_3N coordination in an extended network of bridging thiolate ligands, while in **2** the more sterically hindered penicillamine ligand shaped intertwined polymeric $\{-Ag-(HPen)-\}_n$ strands with linear AgS_2 coordination in a double helix throughout the structure.

Silver(I) complexes formed with cysteine, penicillamine, and glutathione in alkaline aqueous solution were investigated using Ag K-edge EXAFS and ^{109}Ag NMR spectroscopic techniques. In Ag(I)−glutathione solutions with L/Ag mole ratios 2.0−10.0 at $C_{Ag(I)}$ = 0.01 mol dm^{-3} (pH ∼11), mononuclear $[Ag(Glu)_2]^{5-}$ species formed with digonal AgS_2 coordination at all ligand concentrations. The mean Ag−S bond distance of 2.36 ± 0.02 Å is established from the solutions containing excess glutathione.

In alkaline cysteine solutions (pH 10−11) containing $C_{Ag(I)}$ ≈ 0.1 mol dm^{-3}, AgS_3 is the main coordination environment, since for all L/Ag mole ratios, 2.0−10.1, a mean Ag−S bond distance of 2.45 ± 0.02 Å consistently emerged. This conclusion was further supported by ^{109}Ag NMR spectroscopy on a concentrated solution ($C_{Ag(I)}$ = 0.8 and C_{H_2Cys} = 1.75 mol dm^{-3}, L/Ag = 2.2), for which the mean Ag−S distance 2.47 ± 0.02 Å and $\delta(^{109}Ag)$ 1103 ppm were obtained. An Ag···Ag distance of 2.92−3.00 Å was obtained from EXAFS model fitting of these solutions, which is consistent with presence of some singly bridged $S_2Ag-(S)-AgS_2$ interactions within oligomeric species with trigonal AgS_3 coordination, as found in **1**.

For the Ag(I)−penicillamine solutions ($C_{Ag(I)}$ ≈ 0.1 mol dm^{-3}, pH 9.0), the mean Ag−S bond distance from EXAFS model fitting increased from 2.40 to 2.44 ± 0.02 Å with increasing L/Ag mole ratios from 2.0 to 10.0, suggesting that some amount of species with AgS_3 coordination gradually formed together with the prevailing AgS_2 coordinated complexes. For a concentrated solution with L/Ag = 2.0 ($C_{Ag(I)}$ = 0.5 and C_{H_2Pen} = 1.0 mol dm^{-3}), the ^{109}Ag NMR chemical shift of 922 ppm and mean Ag−S distance of 2.40 ± 0.02 Å support that Ag(I)−penicillamine species with AgS_2 coordination still dominate.

The concentration of silver (10−100 mmol dm^{-3}) and also the pH (9−11) used in the current study do not represent the conditions at the cellular level (pH ∼7.4). However, they provides complementary structural information to the potentiometric study by Adams and Kramer,[37] which was carried out with low total Ag(I) and cysteine/glutathione concentrations ($c_L = 10^{-6}-10^{-1}$ mol dm^{-3}) over the pH range 4−8. Their study proposed that both cysteine and glutathione coordinate via their thiolate groups in AgL and AgL_2 complexes and that the complex formation is not affected by changes in the degree of protonation of other functional groups: i.e., the deprotonated amine group of these ligands does not play an essential role in the coordination to the Ag(I) atom. The higher free thiolate concentration in the alkaline solutions of the current study promotes formation of higher complexes: for cysteine the Ag(I)−cysteinate 1/3 complex that was not identified in Adams and Kramer's study and for glutathione the $[Ag(Glu)_2]^{5-}$ species.

Our results provide structural information that may assist in describing the silver(I) coordination in complex compounds that form at physiological pH, such as yeast Ag(I)−metallothionein (Ag_8MT), with AgS_2 and AgS_3 sites that were previously characterized by ^{109}Ag NMR spectroscopy,[52,75] and rabbit liver Ag(I)-metallothionein ($Ag_{12}MT$ and $Ag_{17}MT$), which was studied by S K-edge EXAFS spectroscopy.[74] It is evident from the present results that the strong tendency of the thiolate sulfur atom to form bridges between silver(I) ions, balanced by the steric hindrance of the ligand, plays a decisive role in the coordination environment of the Ag(I) thiolate complexes in the solid state and also in solution, which is in line with the structural principles summarized by Dance and co-workers.[22]

ASSOCIATED CONTENT

Supporting Information

Tables, figures, and a CIF file giving a survey of structurally characterized silver(I) complexes with *S*-donor ligands and AgS_2, $AgS_2(N/O)$, and AgS_3 coordination from the Cambridge Structure Database (CSD), crystal structures of **1** and **2**, EXAFS model curve fitting for solutions P and Q, additional curve-fitting results for EXAFS spectra of solutions A, F, P, and Q including the Ag−(N/O) path, and a comparison between EXAFS spectra for the series of Ag(I) solutions containing cysteine (A−E), penicillamine (F−J) and glutathione (K−O), as well as solutions A and P. This material is available free of charge via the Internet at http://pubs.acs.org.

AUTHOR INFORMATION

Corresponding Author

*E-mail for F.J.: faridehj@ucalgary.ca.

Notes

The authors declare no competing financial interest.

ACKNOWLEDGMENTS

X-ray absorption measurements were carried out at the Photon Factory, Tsukuba, Japan (proposal no. 2003G286), and Stanford Synchrotron Radiation Light source (SSRL), which

is operated by the Department of Energy, Office of Basic Energy Sciences, United States. The SSRL Biotechnology Program is supported by the National Institutes of Health, National Center for Research Resources, Biomedical Technology Program, and by the Department of Energy, Office of Biological and Environmental Research (proposal no. 2848). We gratefully acknowledge the Natural Sciences and Engineering Council (NSERC) of Canada, the Canadian Foundation for Innovation (CFI), and the Alberta Science and Research Investment Program (ASRIP) for providing financial support.

REFERENCES

(1) Klasen, H. J. *Burns* **2000**, *26*, 117−130.
(2) Klasen, H. J. *Burns* **2000**, *26*, 131−138.
(3) Edwards-Jones, V. *Lett. Appl. Microbiol.* **2009**, *49*, 147−152.
(4) Atiyeh, B. S.; Costagliola, M.; Hayek, S. N.; Dibo, S. A. *Burns* **2007**, *33*, 139−148.
(5) Gordon, O.; Slenters, T. V.; Brunetto, P. S.; Villaruz, A. E.; Sturdevant, D. E.; Otto, M.; Landmann, R.; Fromm, K. M. *Antimicrob. Agents Chemother.* **2010**, *54*, 4208−4218.
(6) Castellano, J. J.; Shafii, S. M.; Ko, F.; Donate, G.; Wright, T. E.; Mannari, R. J.; Payne, W. G.; Smith, D. J.; Robson, M. C. *Int. Wound J.* **2007**, *4*, 114−122.
(7) Jain, J.; Arora, S.; Rajwade, J. M.; Omray, P.; Khandelwal, S.; Paknikar, K. M. *Mol. Pharm.* **2009**, *6*, 1388−1401.
(8) Rhim, J.-W.; Hong, S.-I.; Park, H.-M.; Ng, P. K. W. *J. Agric. Food Chem.* **2006**, *54*, 5814−5822.
(9) Liau, S. Y.; Read, D. C.; Pugh, W. J.; Furr, J. R.; Russell, A. D. *Lett. Appl. Microbiol.* **1997**, *25*, 279−283.
(10) Sondi, I.; Salopek-Sondi, B. *J. Colloid Interface Sci.* **2004**, *275*, 177−182.
(11) Yoon, K.-Y.; Hoon Byeon, J.; Park, J.-H.; Hwang, J. *Sci. Total Environ.* **2007**, *373*, 572−575.
(12) Cho, K.-H.; Park, J.-E.; Osaka, T.; Park, S.-G. *Electrochim. Acta* **2005**, *51*, 956−960.
(13) Morones, J. R.; Elechiguerra, J. L.; Camacho, A.; Holt, K.; Kouri, J. B.; Ramírez, J. T.; Yacaman, M. J. *Nanotechnology* **2005**, *16*, 2346−2353.
(14) Bradford, A.; Handy, R. D.; Readman, J. W.; Atfield, A.; Mulhling, M. *Environ. Sci. Technol.* **2009**, *43*, 4530−4536.
(15) Xiu, Z.-m.; Zhang, Q.-b.; Puppala, H. L.; Colvin, V. L.; Alvarez, P. J. J. *Nano Lett.* **2012**, *12*, 4271−4275.
(16) Taglietti, A.; Diaz Fernandez, Y. A.; Amato, E.; Cucca, L.; Dacarro, G.; Grisoli, P.; Necchi, V.; Pallavicini, P.; Pasotti, L.; Patrini, M. *Langmuir* **2012**, *28*, 8140−8148.
(17) Ghandour, W.; Hubbard, J. A.; Deistung, J.; Hughes, M. N.; Poole, R. K. *Appl. Microbiol. Biotechnol.* **1988**, *28*, 559−565.
(18) Liu, J.; Sonshine, D. A.; Shervani, S.; Hurt, R. H. *ACS Nano* **2010**, *4*, 6903−6913.
(19) Tang, K.; Aslam, M.; Block, E.; Nicholson, T.; Zubieta, J. *Inorg. Chem.* **1987**, *26*, 1488−1497.
(20) Dance, I. G.; Fisher, K. J.; Banda, R. M. H.; Scudder, M. L. *Inorg. Chem.* **1991**, *30*, 183−187.
(21) Dance, I. G.; Fitzpatrick, L. J.; Rae, A. D.; Scudder, M. L. *Inorg. Chem.* **1983**, *22*, 3785−3788.
(22) Dance, I. G.; Fitzpatrick, L. J.; Craig, D. C.; Scudder, M. L. *Inorg. Chem.* **1989**, *28*, 1853−1861.
(23) Block, E.; Gernon, M.; Kang, H.; Ofori-Okai, G.; Zubieta, J. *Inorg. Chem.* **1989**, *28*, 1263−1271.
(24) Perez-Lourido, P.; Garcia-Vazquez, J. A.; Romero, J.; Sousa, A.; Block, E.; Maresca, K. P.; Zubieta, J. *Inorg. Chem.* **1999**, *38*, 538−544.
(25) Howard-Lock, H. E. *Metal-Based Drugs* **1999**, *6*, 201−209.
(26) Allen, F. H. *Acta Crystallogr., Sect. B* **2002**, *B58*, 380−388.
(27) Bell, R. A.; Bennett, S.; Britten, J. F.; Hu, M. In *The 5th International Conference Proceedings: Transport, Fate and Effects of Silver in the Environment*, Hamilton, ON, Canada, Sept 28−Oct 1, 1997; Andren, A. W., Bober, T. W., Eds.; University of Wisconsin System/Sea Grant Institute: 1997; pp 13−18.
(28) Bell, R. A.; Kramer, J. R. *Environ. Toxicol. Chem.* **1999**, *18*, 9−22.
(29) Zegzhda, G. D.; Zegzhda, T. V.; Shulman, V. M. *Russ. J. Inorg. Chem.* **1969**, *14*, 70−73.
(30) Ahmad, S.; Hanif, M.; Monim-ul-Mehboob, M.; Isab, A. A.; Ahmad, S. *Synth. React. Inorg. Met.-Org. Nano-Met. Chem.* **2009**, *39*, 45−49.
(31) Costa, G. S. M.; Corbi, P. P.; Abbehausen, C.; Formiga, A. L. B.; Lustri, W. R.; Cuin, A. *Polyhedron* **2012**, *34*, 210−214.
(32) Kasuga, N. C.; Yoshikawa, R.; Sakai, Y.; Nomiya, K. *Inorg. Chem.* **2012**, *51*, 1640−1647.
(33) Abbehausen, C.; Heinrich, T. A.; Abrão, E. P.; Costa-Neto, C. M.; Lustri, W. R.; Formiga, A. L. B.; Corbi, P. P. *Polyhedron* **2011**, *30*, 579−583.
(34) Tunaboylu, K.; Schwarzenbach, G. *Helv. Chim. Acta* **1971**, *54*, 2166−2185.
(35) Andersson, L.-O. *J. Polym. Sci., Part A1* **1972**, *10*, 1963−1973.
(36) Tseng, P. K. C.; Gutknecht, W. F. *Anal. Chem.* **1975**, *47*, 2316−2319.
(37) Adams, N. W. H.; Kramer, J. R. *Aquat. Geochem.* **1999**, *5*, 1−11.
(38) Alekseev, V.; Semenov, A.; Pakhomov, P. *Russ. J. Inorg. Chem.* **2012**, *57*, 1041−1044.
(39) Mah, V.; Jalilehvand, F. *Chem. Res. Toxicol.* **2010**, *23*, 1815−1823.
(40) Mah, V.; Jalilehvand, F. *J. Biol. Inorg. Chem.* **2010**, *15*, 441−58.
(41) Jalilehvand, F.; Leung, B. O.; Mah, V. *Inorg. Chem.* **2009**, *48*, 5758−5771.
(42) Jalilehvand, F.; Mah, V.; Leung, B. O.; Mink, J.; Bernard, G. M.; Hajba, L. *Inorg. Chem.* **2009**, *48*, 4219−4230.
(43) Jalilehvand, F.; Leung, B. O.; Izadifard, M.; Damian, E. *Inorg. Chem.* **2006**, *45*, 66−73.
(44) Mah, V.; Jalilehvand, F. *J. Biol. Inorg. Chem.* **2008**, *13*, 541−53.
(45) Leung, B. O.; Jalilehvand, F.; Mah, V. *Dalton Trans.* **2007**, 4666−4674.
(46) Harris, R. K.; Becker, E. D.; Cabral de Menezes, S. M.; Goodfellow, R.; Granger, P. *Pure Appl. Chem.* **2001**, *73*, 1795−1818.
(47) Henrichs, P. M., Silver-109. In *NMR of Newly Accessible Nuclei*; Laszlo, P., Ed.; Academic Press: New York, 1983; Vol. 2 (Chemically and Biochemically Important Elements), Chapter 12, pp 319−336.
(48) Penner, G. H.; Li, W. *Inorg. Chem.* **2004**, *43*, 5588−5597.
(49) Penner, G. H.; Liu, X. *Prog. Nucl. Magn. Reson. Spectrosc.* **2006**, *49*, 151−167.
(50) Bowmaker, G. A.; Harris, R. K.; Assadollahzadeh, B.; Apperley, D. C.; Hodgkinson, P.; Amornsakchai, P. *Magn. Reson. Chem.* **2004**, *42*, 819−826.
(51) Nilsson, K. B.; Persson, I.; Kessler, V. G. *Inorg. Chem.* **2006**, *45*, 6912−6921.
(52) Narula, S. S.; Mehra, R. K.; Winge, D. R.; Armitage, I. M. *J. Am. Chem. Soc.* **1991**, *113*, 9354−9358.
(53) Henrichs, P. M.; Ackerman, J. J. H.; Maciel, G. E. *J. Am. Chem. Soc.* **1977**, *99*, 2544−2548.
(54) Merwin, L. H.; Sebald, A. *J. Magn. Reson.* **1992**, *97*, 628−631.
(55) Hooft, R. *COLLECT: User's Manual*; Nonius BV: Delft, The Netherlands, 1998.
(56) Otwinowski, Z.; Minor, W. Processing of X-ray diffraction data collected in oscillation mode. In *Methods in Enzymology*; Carter, C. W., Jr., Sweet, R. M., Eds.; Academic Press: New York, 1997; Vol. *276* (Macromolecular Crystallography, part A), pp 307−326.
(57) Altomare, A.; Cascarano, G.; Giacovazzo, C.; Guagliardi, A. *J. Appl. Crystallogr.* **1993**, *26*, 343−350.
(58) Beurskens, P. T.; Admiraal, G.; Beurskens, G.; Bosman, W. P.; de Gelder, R.; Israel, R.; Smits, J. M. M. *The DIRDIF-94 program system, Technical Report of the Crystallography Laboratory*; University of Nijmegen, Nijmegen, The Netherlands, 1994.
(59) Sheldrick, G. M. *SHELXL97-A Program for Refinement of Crystal Structures*; University of Göttingen, Göttingen, Germany, 1997.
(60) Brevard, C.; Granger, P. *Handbook of High Resolution Multinuclear NMR*; Wiley & Sons: New York, 1981.
(61) Oyanagi, H.; Matsushita, T.; Ito, M.; Kuroda, H. *KEK Rep.* **1984**, *83*−*30*, 1−27.

(62) George, G. N.; George, S. J.; Pickering, I. J. *EXAFSPAK*; Stanford Synchrotron Radiation Lightsource (SSRL), Menlo Park, CA, 2001.
(63) Ressler, T. *J. Synchrotron Radiat.* **1998**, *5*, 118−122.
(64) Ankudinov, A. L.; Rehr, J. J. *Phys. Rev. B* **1997**, *56*, R1712−R1716.
(65) Zabinsky, S. I.; Rehr, J. J.; Ankudinov, A.; Albers, R. C.; Eller, M. J. *Phys. Rev. B* **1995**, *52*, 2995−3009.
(66) Singh, K.; Long, J. R.; Stavropoulos, P. *J. Am. Chem. Soc.* **1997**, *119*, 2942−2943.
(67) Bondi, A. *J. Phys. Chem.* **1964**, *68*, 441−451.
(68) Wang, H. M. J.; Lin, I. J. B. *Organometallics* **1998**, *17*, 972−975.
(69) Baenziger, N. C.; Struss, A. W. *Inorg. Chem.* **1976**, *15*, 1807−1809.
(70) El-Bahraoui, J.; Molina, J.; Olea, D. P. *J. Phys. Chem. A* **1998**, *102*, 2443−2448.
(71) Zhou, Y.; Chen, W.; Wang, D. *Dalton Trans.* **2008**, 1444−1453.
(72) Jansen, M. *Angew. Chem., Int. Ed. Engl.* **1987**, *26*, 1098−1110.
(73) Fujisawa, K.; Imai, S.; Moro-oka, Y. *Chem. Lett.* **1998**, 167−168.
(74) Gui, Z.; Green, A. R.; Kasrai, M.; Bancroft, G. M.; Stillman, M. J. *Inorg. Chem.* **1996**, *35*, 6520−6529.
(75) Narula, S. S.; Winge, D. R.; Armitage, I. M. *Biochemistry* **1993**, *32*, 6773−6787.
(76) Fijolek, H. G.; Oriskovich, T. A.; Benesi, A. J.; Gonzalez-Duarte, P.; Natan, M. J. *Inorg. Chem.* **1996**, *35*, 797−799.
(77) Fijolek, H. G.; Grohal, J. R.; Sample, J. L.; Natan, M. J. *Inorg. Chem.* **1997**, *36*, 622−628.
(78) Jalilehvand, F.; Amini, Z.; Parmar, K. *Inorg. Chem.* **2012**, *51*, 10619−10630.
(79) Fijolek, H. G.; González-Duarte, P.; Park, S. H.; Suib, S. L.; Natan, M. J. *Inorg. Chem.* **1997**, *36*, 5299−5305.
(80) Nomiya, K.; Kondoh, Y.; Onoue, K.; Kasuga, N. C.; Nagano, H.; Oda, M.; Sudoh, T.; Sakuma, S. *J. Inorg. Biochem.* **1995**, *58*, 255−267.
(81) Nomiya, K.; Onoue, K.-I.; Kondoh, Y.; Kasuga, N. C.; Nagano, H.; Oda, M.; Sakuma, S. *Polyhedron* **1995**, *14*, 1359−1367.